Fast evaluation of transient acoustic fields

Michael Carley[a)]
Department of Mechanical Engineering, University of Bath, Bath BA2 7AY, United Kingdom

(Received 24 August 2015; revised 26 November 2015; accepted 12 January 2016; published online 4 February 2016)

The efficient computation of transient fields radiated by non-harmonic source distributions is a problem relevant in numerous areas of acoustics. This paper presents an efficient easily implemented method for the generation of time-dependent spherical harmonic expansions for arbitrary sources, which can be used to compute the transient radiated field at arbitrary points outside the source domain. The method depends on the theory of time-domain spherical harmonic expansions and the solution of Vandermonde systems. Results are presented demonstrating the efficiency and accuracy of the method with respect to full evaluation of the field radiated by a randomized source distribution. © *2016 Acoustical Society of America*. [http://dx.doi.org/10.1121/1.4941251]

[NAG] Pages: 630–635

I. INTRODUCTION

It is common in acoustic simulations to wish to compute the field radiated into some large region. This may be necessary as input to a scattering or propagation calculation, as a visualization technique, or simply because there is a requirement to assess noise levels at many positions. While there exist approaches that allow a radiated field to be computed efficiently in the frequency domain, techniques for the fast computation of transient fields are not so well developed. In this paper, we present a simple approach that generates time-domain spherical harmonic expansions for the acoustic field using only standard computation techniques as input. These expansions can be used to accurately and efficiently compute the field at arbitrary points outside a source region, and also allow the source to be represented by a relatively small number of coefficients, reducing the computer memory required.

The use of spherical harmonic expansions is not new, and they are a widely used tool in frequency domain methods. In the time domain, they are not so common, but they have been used for field computation in a number of physical applications including electromagnetism[1,2] and acoustics.[3,4] In acoustics, the spherical harmonic expansion has been used as a means to characterize a source using physical data,[4] by measuring the acoustic pressure on a spherical surface containing the source, and applying deconvolution operations to find the coefficients of the expansion. In the electromagnetism literature,[2] the coefficients have been computed directly from the source distribution in order to generate an expansion that can be used to evaluate the radiation field of an antenna.

Given the importance of computing transient wave fields, a number of other methods have been presented for the problem, for example, plane wave expansion,[5] filtered convolution,[6] and a specialized iterative procedure.[7,8] While each of these techniques has its strengths, they typically suffer from complexity in implementation, or do not offer a very large improvement in computational performance.

It is worth considering the scale of the computational problem to be dealt with. Margnat and Fortuné[8] deal with a problem of computing noise from a two-dimensional mixing layer. In their calculation, there are 1.6×10^6 source points and the field is computed for 755 time points at 2.3×10^4 observer points. Note that this is a two-dimensional problem with the radiated noise computed in a relatively small region around the source. Even then, the calculation becomes computationally expensive if it is conducted using direct integration over the source for each field point separately.

Similar considerations apply in more general cases: if the field is to be adequately resolved on the scale of the shortest wavelength present λ, the number of evaluation points increases as $(L/\lambda)^2$ for calculations on a plane, or $(L/\lambda)^3$ if the field is required throughout a volume, where L is a characteristic dimension of the radiation region rather than of the source. If the frequency content of the transient signal is to be properly captured, the sampling frequency scales as c/λ, where c is speed of sound, so that the number of time points is proportional to cT/λ, where T is the length of the transient signal and the total computational effort can scale as cTL^3/λ^4, or $f^4(L/c)^3T$, where f is the frequency corresponding to the shortest wavelength, in effect, the transient signal bandwidth.

Clearly, efficient techniques for source data compression and field evaluation are required. Ideally, these techniques will fit readily into existing computational frameworks, and will not introduce unnecessary extra complexity.

The method presented in this paper is based on the same theoretical ideas as previous work employing spherical harmonics, but is simpler to implement computationally, and is based directly on the theory of time-domain spherical harmonics. The problem can be stated as follows: given a source distribution contained within a sphere of radius r, generate a time-dependent spherical harmonic expansion that gives the same radiated field outside the source region as the original source does. Our basic theory is that of Heyman and Devaney[9] who give a number of approaches to

[a)]Electronic mail: m.j.carley@bath.ac.uk

the time-dependent multipole problem, viewed as a characterization of a source distribution, or as a property of a radiated field. The resulting technique is easily implemented using free software,[10,11] and can use any convenient method for field evaluation to generate input data, as the approach is based purely on properties of the acoustic field.

The use of spherical harmonics makes no assumption about the nature of the source other than that it be contained inside some volume of finite radius, but it is worth considering the types of source to be encountered in applications. Broadly, these break down into volume sources such as jets,[7,8] surface sources such as scattering bodies and rotors,[12] and, a subset of surface sources, Kirchhoff surface sources, which are used to project an acoustic field defined by flow data into the acoustic field.[13] In practice, volume sources are likely to be the most numerically intensive given that they will have the largest number of computational elements contributing to the field.

We note that while no assumption is made about the nature of the sources, as long as their acoustic field can be computed, in practice, elementary sources of order higher than quadrupole are not likely to arise in applications, although the effects of interference and source motion may well make the field higher order. We also note that, unlike calculations in the frequency domain, time domain calculations are not accelerated by applying a far-field approximation, since the most time-consuming part of the problem is usually the calculation of retarded time. Finally, a motivation for the approach used in this paper is the automatic satisfaction of the causality requirement, which is preferable for any application involving a time-dependent field, as noted by Heyman and Devaney,[9] especially by comparison to plane-wave methods, which generate a causal field only because of the cancellation of non-causal components, and not because the causality is built into the method.

II. ANALYSIS

The basic arrangement is shown in Fig. 1. The source region is surrounded by a set of spherical layers of radius r_i, $i = 0, \ldots, N$. As part of the method, we assume that a means of computing the field radiated by the source is available, so that the acoustic pressure can be found at any required point on the spherical shells. We adopt spherical polar coordinates (r, θ, ϕ) fixed at the centre of the spheres with $x = r\cos\phi\sin\theta$, $y = r\sin\phi\sin\theta$, $z = r\cos\theta$.

A. Spherical harmonic expansions

Heyman and Devaney[9] show that the time-dependent field outside the source volume can be expressed as

$$p(\mathbf{r}, t) = \frac{1}{4\pi r}\sum_{l=0}^{\infty}\sum_{m=-l}^{l} Y_{l,m}(\hat{\mathbf{r}})\mathcal{L}_l q_{l,m}(\tau), \tag{1}$$

where $\tau = t - r/c$ is the retarded time, and $q_{l,m}(\tau)$ is a time-dependent multipole coefficient, operated on by

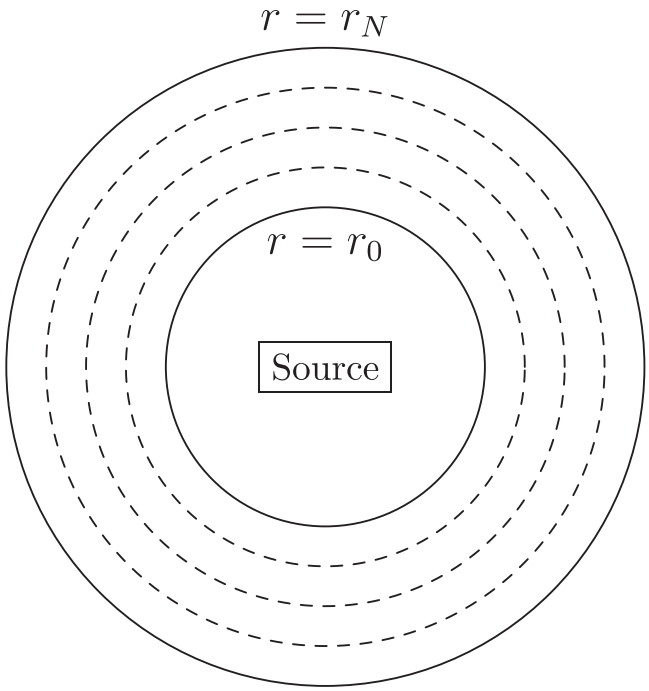

FIG. 1. Source and spherical layers.

$$\mathcal{L}_l = \sum_{n=0}^{l}\frac{(l+n)!}{n!(l-n)!}\left(\frac{c}{2r}\right)^n \partial_\tau^{-n}, \tag{2}$$

with ∂_τ^{-n} denoting an nth order integration, as used in the method of Klinkenbusch.[2] The spherical harmonics are, using the standard normalization,

$$Y_{l,m}(\hat{\mathbf{r}}) = \sqrt{\frac{1}{4\pi}\frac{(2l+1)(l-m)!}{(l+m)!}}P_l^m(\cos\theta)\mathrm{e}^{\mathrm{j}m\phi}, \tag{3}$$

where P_l^m is the associated Legendre function. Rewriting to remove the operator $\mathcal{L}_l$, and truncating to a finite number of terms, we take as our working expansion

$$p(\mathbf{r}, \tau + r/c) \approx \frac{1}{r}\sum_{l=0}^{L}\sum_{m=-l}^{l} Y_{l,m}(\hat{\mathbf{r}})\sum_{n=0}^{l}\frac{q_{l,m}^{(n)}(\tau)}{r^n}, \tag{4}$$

with the moments $q_{l,m}^{(n)}(\tau)$ to be determined by a method described later. Heyman and Devaney[9] demonstrate that these moments, and the field outside the source volume, are completely determined by the time-dependent radiation pattern $p(\mathbf{r}, t)$. Thus, given the field on a suitably chosen set of surfaces, the moments can be computed, and the field at an arbitrary point outside the source region estimated.

B. Computation of multipole moments

The multipole moments $q_{l,m}^{(n)}(\tau_j)$ are computed as follows for each time step τ_j. The acoustic field $p(\mathbf{r}, t)$ is computed on each spherical shell for time $t = \tau_j + r_i/c$. The evaluation points are set by the requirements of the spherical harmonic transform[11] and are specified as (θ_i, ϕ_j), $1 \le i \le N_\theta$, $1 \le j \le N_\phi$, where N_θ is user-specified and constrains the number of spherical multipole coefficients that can be

calculated, with $N_\phi = 2N_\theta$. For each sphere radius, the field is computed on the surface and the spherical harmonic transform is applied, yielding, on the ith surface,

$$r_i \hat{p}^{(i)}_{l,m}(\tau_j) = \sum_{n=0}^{l} \frac{q^{(n)}_{l,m}(\tau_j)}{r_i^n}, \tag{5}$$

where $\hat{p}^{(i)}_{l,m}(\tau_j)$ is the (l, m) coefficient in the spherical harmonic expansion of $p(\tau_j + r_i/c)$ on the surface of radius r_i. The coefficients are found by performing a spherical harmonic transform on the pressure field computed on the spherical surfaces, as in Eq. (4). For $i = 0, \ldots, N$, this yields a system of linear equations for the multipole moments $q^{(n)}_{l,m}(\tau_j)$. This is a Vandermonde system, which is known to be poorly conditioned, but there exists a stable algorithm for its solution that gives very accurate results.[14] Thus, given a set of surfaces enclosing the source region, and a means of computing p on those surfaces at any required t, the time-dependent multipole moments $q^{(n)}_{l,m}(\tau)$ can be found, and hence the radiated field, using Eq. (4).

C. Field calculation

The final stage of the calculation, once the multipole coefficients have been determined is the evaluation of the acoustic pressure at required points in the field. This is implemented using the inverse spherical harmonic transform[11] to evaluate Eq. (4). This gives the contribution of each multipole term at a given retarded time τ. We note that the spherical harmonic transform library of Schaeffer[11] includes a fast-Fourier transform (FFT)-based algorithm for the computation of the field, which gives the field at all sampling points on the spherical shell. While this algorithm is more efficient than the single point method that is also available in the library, it does not necessarily give the field at points required by the user, so our results are reported using the single point method. This increases the reported computation time per field point, but we believe that it gives a more realistic measure of the performance to be expected in applications.

In computing the field at a point $\mathbf{x}$, the retarded time $\tau = |\mathbf{x}|/c$ will not necessarily be equal to one of the sample retarded times τ_j and an interpolation must be performed. This is implemented using an advanced time algorithm,[15] where retarded time τ is fixed and reception time t is computed. We assume that the acoustic signal is to be evaluated at times $t_k = k\Delta t$, where $\Delta t = \Delta\tau$. Then, for retarded time τ_j,

$$t = \tau_j + r/c, \tag{6}$$

where $r = |\mathbf{x}|$. The acoustic pressure at time t_k is then given by the interpolation

$$p(t_k) = \sum_j w_j p(\tau_j + r/c), \tag{7}$$

where the weights w_j are, in this case, given by the Lagrange interpolating polynomials. With $\Delta t \equiv \Delta\tau$, the weights do not vary with t. In the results to be presented, interpolation using Lagrange polynomials up to order three has been tested.

We note here that the temporal interpolation scheme is likely to be the largest source of error in the algorithm: if the coefficients of the expansion are computed using Eqs. (4) and (5) the resulting pressure field is exact, other than for errors caused by truncation of the expansion, at values of time $t = \tau_j + r/c$. Interpolation between these time points, however, introduces errors from interpolation and/or aliasing. Such interpolation is unavoidable in applications, since it is inevitable that the pressure signal will be required on some specified set of time points, and so it is included in the algorithm presented here.

D. Algorithm

The computational algorithm can be summarized as follows.

(1) Pre-processing:
   (a) For each retarded time step τ_j, compute the acoustic field at the sampling points on the spherical shells;
   (b) solve Eq. (5) using the algorithm of Golub and Van Loan[14] to give $q^{(n)}_{l,m}(\tau_j)$.
(2) For each field point of interest, evaluate Eq. (4).

In our implementation, all forward and inverse spherical harmonic transforms are evaluated using the library of Schaeffer.[11]

E. Computational effort

The computational effort of the algorithm is readily estimated. The cost of computing the multipole coefficients is given by $N_M N_s T_f$, where N_M is the number of coefficients, determined by the number of points on each spherical grid and the number of layers used, N_s is the number of sources, and T_f is the computational cost of calculating the field due to one source at one field point. We assume that the computation time for the spherical harmonic transform is negligible, an assumption partly justified by the use of the FFT to accelerate the calculation and by limiting the number of terms used in the spherical harmonic expansion. The computational cost of computing the acoustic signal at one field point is given by $T_M N_M$, where T_M is the time required to compute the field from one spherical harmonic coefficient.

On these assumptions, we can estimate the number of field points N_f at which the computational cost of the multipole method, including the setup time, breaks even with the direct calculation, from

$$N_M N_s T_f + N_M N_f T_M = N_s N_f T_f,$$

$$N_f = \frac{N_M N_s T_f}{N_s T_f - N_M T_M}, \tag{8}$$

and for $N_s \gg N_M$, the case of interest in a real application, the multipole expansion becomes faster than direct calculation at $N_f \approx N_M$.

This estimate of computational effort depends on limiting the number of spherical harmonic coefficients used, with

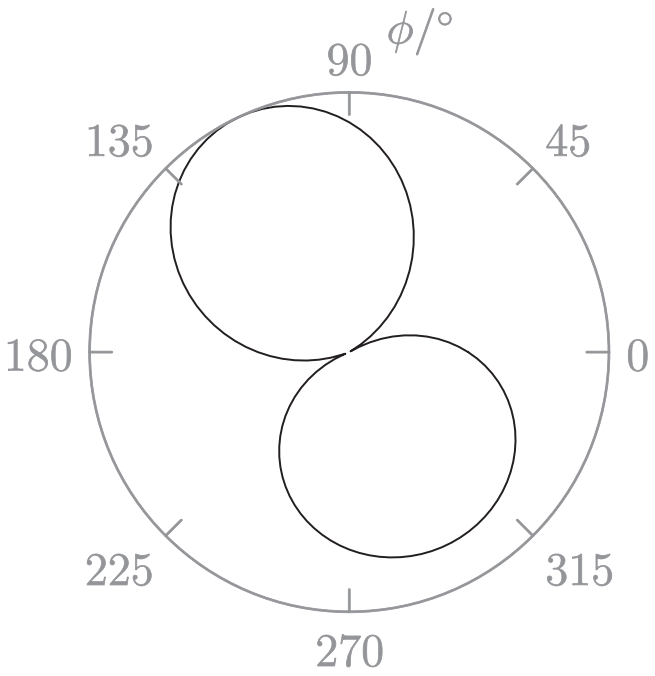

FIG. 2. Directivity of test field in plane $z=0$ at frequency $\omega=\Omega$, $r=5/2$, scaled on maximum amplitude.

that number being a function of the discretization of the spherical shells and of their radii. The selection of these surfaces is constrained by the need to avoid spatial aliasing, which translates into a constraint on the spatial separation of sampling points as a function of minimum wavelength of the signal, or equivalently signal bandwidth.

III. SAMPLE CALCULATIONS

We present a set of results to demonstrate the accuracy of the computation method, and to investigate the computational effort. As a test input, we use N_s dipole point sources distributed randomly in a sphere of radius 1/8, with positions $\mathbf{y}_n$ and random vector amplitudes $\mathbf{a}_n$. Our aim is to use a source term with parameters that can be varied systematically, in order to investigate the effect on error and computation time, and which is reasonably representative of the directional volume sources for which the method is most likely to be useful, such as turbulent flows. The time variation of the sources is given by a wavepacket function and the resulting field is

$$p(\mathbf{x},t)=\sum_{n=1}^{N_s}\frac{\mathbf{a}_n.\mathbf{r_n}}{4\pi|\mathbf{r}_n|^2}\left[\frac{q(\tau_n)}{|\mathbf{r}_n|}+\frac{\dot{q}(\tau_n)}{c}\right],$$
$$\mathbf{r}_n=\mathbf{x}-\mathbf{y}_n,\quad \tau_n=t-|\mathbf{r}_n|/c,$$
$$q(\tau)=\mathrm{e}^{-\tau^2/\sigma^2}\cos\Omega\tau. \qquad (9)$$

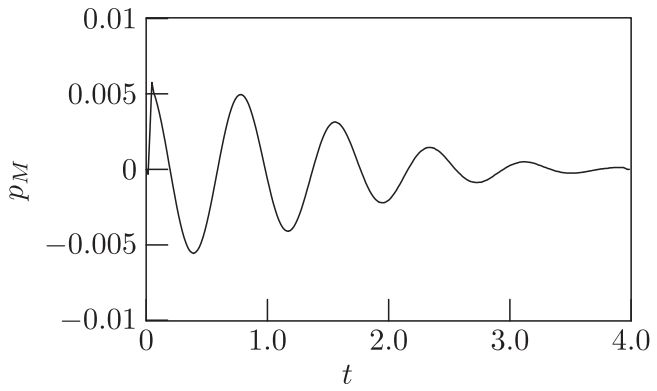

FIG. 3. Computed signal for test case of Eq. (9), $N_s=128$.

The dipole amplitudes $\mathbf{a}_n$ are set randomly with each component of $\mathbf{a}_n$ lying between -1 and 1. The use of a wavepacket source $q(\tau)$ tests the method on an oscillatory non-periodic source, while the use of random source amplitudes introduces partial cancellation effects that modify the directivity of the radiated field. The error measure is

$$\epsilon_{\mathrm{rms}}=\left[\overline{(p_M-p)^2}\right]^{1/2}, \qquad (10)$$

where p_M is the acoustic signal computed using the multipole expansion, and p is calculated directly from Eq. (9). A relative error measure has not been used because the instantaneous total source strength is approximately zero.

Results for computation time and error are given on log scales to the base two, in order to show the rate of doubling (halving) of computation time (error) with doubling of the number of sources or other relevant quantities.

As an illustration of the nature of the acoustic field that is being modeled, Fig. 2 shows a polar plot against ϕ in the plane $z=0$ of the directivity of the field at the underlying frequency Ω of the wavepacket, showing that the net field is approximately, but not exactly, dipole, with a tilted axis.

A. Single point test

As a first test to demonstrate the performance of the technique, including where it begins to break down, we compute the field at a single point with various combinations of computational parameters. Data presented are error ϵ_{rms}, computation time T_q for the coefficients $q_{l,m}^{(n)}(\tau)$, and the computation times T_M and T_D per field point for the multipole and direct methods, respectively. Results are given as a function of number of source points, number of multipole coefficients, and the order of temporal interpolation in Eq. (7). For the computations, $\Omega=8$, $\sigma=2$, and $\Delta t=1/64$.

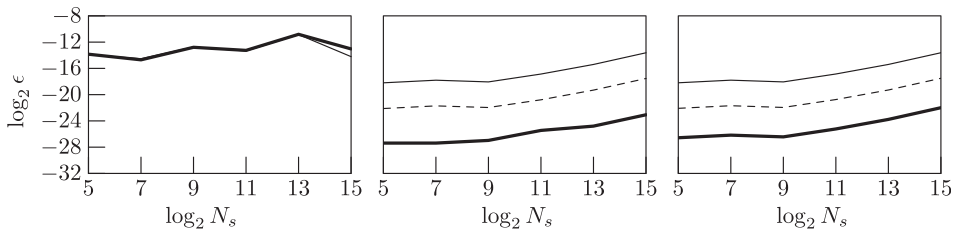

FIG. 4. Error as a function of number of sources and interpolation order. Plot a, $N_\theta=4$; plot b, $N_\theta=8$; plot c, $N_\theta=12$: solid line first-order; dashed line second-order; bold line third-order temporal interpolation.

The choice of shell radii for the surfaces bounding the source is to some degree under the control of the user. To our knowledge, there is no optimal choice of entries for a Vandermonde matrix, so the shell radii were chosen to give equal intervals in $1/r$,

$$r_i = \frac{1}{1/r_{\max} + i\Delta(1/r)}, \tag{11}$$

with $r_{\max} = 2$ and $\Delta(1/r) = 1/8$.

Figure 3 shows a sample signal computed using the multipole expansion. The transients at the start and end of the signal should be noted. These arise because of the absence of source data for $\tau < 0$ and $\tau > 4$ and their length depends on the order of interpolation scheme used.

Error in the computed field is presented in Fig. 4 as a function of the order of interpolation, N_θ and N_s. The number of spherical shells is N_θ, a value chosen to make Eq. (5) well-posed. The resulting number of points on the spherical layers is then $N_M = 2N_\theta^3$, determined by the requirements of the spherical harmonic transform[11] and the number of layers used.

The error appears to be controlled by two factors. In the first plot, $N_\theta = 4$, the error is independent of interpolation order and of N_s. This seems to be because there are insufficient spherical harmonics in the expansion to accurately capture the field, and this lack of coefficients dominates the other effects. In the second and third plots, however, the error is much lower and varies with interpolation order, as might be expected. The increase in root-mean-square (rms) error with number of sources appears to be caused by the lack of normalization in the error measure. Given that the total instantaneous source strength is approximately zero, there is no obvious scaling term that could be used to normalize the error with number of sources, so the total rms error in the computed signal has been retained, with the caveat about absolute error measure increasing with source number.

The first plot in Fig. 5 shows the computation time for calculation of the multipole coefficients, and for the pressure at one field point by the multipole and the direct approach, each scaled on the time for direct calculation at the smallest N_s, with $N_\theta = 8$ ($N_M = 1024$). As expected the multipole setup and the direct approach have computational times that scale as N_s, giving lines that are parallel on the time plot,

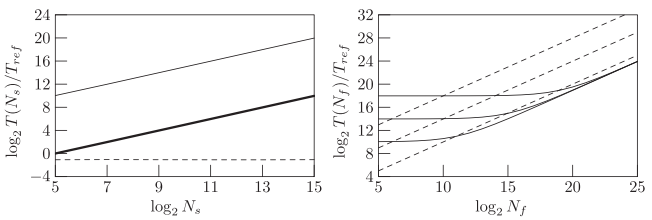

FIG. 5. Computation times for direct and multipole calculations, $N_\theta = 8$, third-order temporal interpolation. Left-hand plot: solid line, setup time for multipole coefficients; bold line, direct calculation for one field point; dashed line: multipole calculation for one field point. Right-hand plot: total computation time for $N_s = 2^5$, top to bottom, $N_f = 2^{13}, 2^9, 2^5$; solid lines, multipole calculation including setup time; dashed lines, direct calculation. All computation times scaled on T_{ref} direct calculation time for one field point with $N_s = 2^5$.

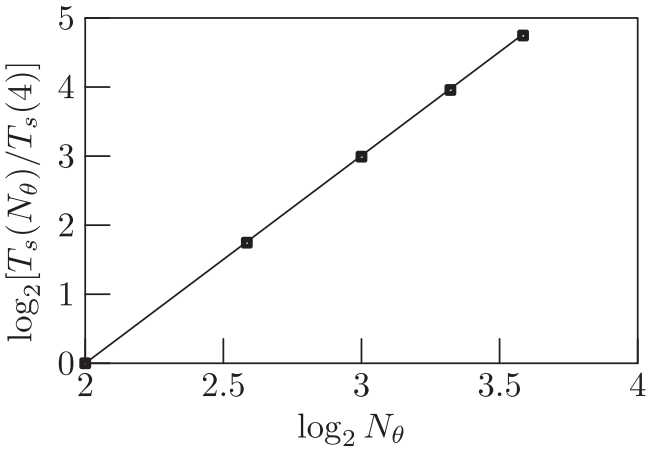

FIG. 6. Setup time T_s against N_θ, scaled on T_s for $N_\theta = 4$: symbols, $T_s/T_s(4)$; solid line N_θ^3 fit.

while the time for multipole calculation of the pressure at one field point is constant with N_s. The second plot in Fig. 5 shows the total computation time as a function of number of field points N_f for three different values of N_s, 2^5, 2^9, and 2^{13}. The computation times for direct calculation, shown as dashed lines, increase steadily with N_f as expected, while the multipole calculations require a greater time at small N_f, reflecting the setup cost, but asymptote to a straight line independent of N_s at large N_f, as the setup cost loses significance in the overall computational time. The break-even point, where the dashed lines cross the solid curves, is indeed at $N_f \approx 2^{10} = 1024 = N_M$ as predicted by Eq. (8).

To examine the dependence of setup time on the sampling resolution of the field, Fig. 6 shows the variation of setup time with N_θ. As expected from the computational effort required for the underlying spherical harmonic transform algorithm,[11] the time scales as N_θ^3. If a maximum value of N_θ is imposed, to keep the computation time manageable,

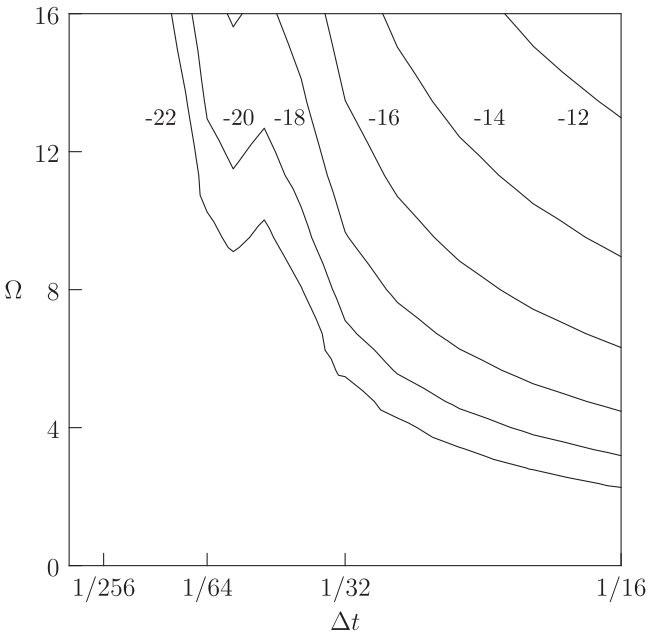

FIG. 7. Variation of error $\log_2 \epsilon_{\text{rms}}$ with time step Δt and frequency Ω with third-order interpolation, $N_s = 2^{10}$; other parameters as for Fig. 5.

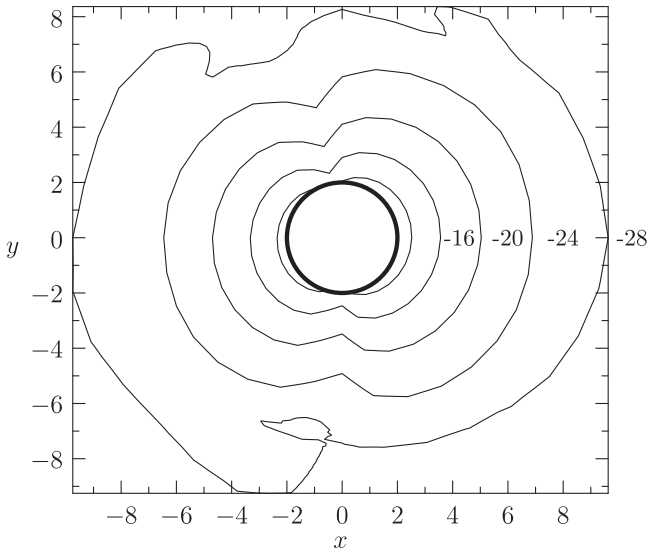

FIG. 8. Error in plane $z=0$, $-28 \leq \log_2 \epsilon_{\text{rms}} \leq -12$, in steps of 4; bold line outer spherical harmonic surface.

this sets a maximum radius for the spherical shells in order to avoid spatial aliasing for signals of a given temporal bandwidth. In practice, this problem would be dealt with by breaking the source distribution into smaller regions each of which can be handled by a multipole expansion of reasonable size.

As a check on the sensitivity of the method to time step and signal bandwidth, Fig. 7 shows absolute error computed as a function of Δt and Ω. Other parameters are set to the same values as in Fig. 5 with $N_s = 1024$ and third-order interpolation in time. As might be expected, the plot shows a relatively large error for larger time steps and higher frequencies, with the error reducing with Δt and/or Ω. The larger error appears to be introduced by an inability of the Lagrangian scheme to accurately interpolate when the time step is too large, corresponding to an aliasing effect.

B. Full field results

The purpose of the method presented here is the fast evaluation of data at multiple points in a field. As a check on variation of error with field position, Fig. 8 shows computed error in a region of the plane $z=0$ around the source bounded by $r=2$. The error in the region varies from about 2^{-8} to 2^{-32} and decays rapidly away from the source boundary.

IV. CONCLUSIONS

We have presented a method for the generation of time-domain spherical harmonic expansions that can be used in the fast evaluation of transient acoustic fields outside a source region. The method has been tested on randomized source distributions with a marked directivity and has been found accurate and efficient. Future work will consider the use of the technique on source distributions that are decomposed into smaller distributions as a step towards a fast time-domain radiation method for arbitrary source geometries. A further interesting question is whether there exists an optimal set of nodes for Vandermonde systems, i.e., optimal radii for the spherical shells used to generate the spherical harmonic expansion.

[1]J. Adam and L. Klinkenbusch, "Efficient evaluation of antenna fields by a time-domain multipole analysis," Adv. Radio Sci. **7**, 43–48 (2009).
[2]L. Klinkenbusch, "Time domain near-field to near-field transformation using a spherical-multipole approach," Radio Sci. **46**, 1–8, doi:10.1029/2011RS004670 (2011).
[3]O. M. Buyukdara and S. Sencer Koc, "Two alternative expressions for the spherical wave expansion of the time domain scalar free-space Green's function and an application: Scattering by a soft sphere," J. Acoust. Soc. Am. **101**(1), 87–91 (1997).
[4]S. Sencer Koc, A. Civi, and O. M. Buyukdara, "Near-field scanning in the time domain on a spherical surface—A formulation using the free-space Green's function," J. Acoust. Soc. Am. **110**(4), 1778–1782 (2001).
[5]A. Arif Ergin, B. Shanker, and E. Michielssen, "Fast evaluation of three-dimensional transient wave fields using diagonal translation operators," J. Comput. Phys. **146**, 157–180 (1998).
[6]M. D. Verweij and J. Huijssen, "A filtered convolution method for the computation of acoustic wave fields in very large spatiotemporal domains," J. Acoust. Soc. Am. **125**(4), 1868–1878 (2009).
[7]F. Margnat, "A fast procedure for the computation of acoustic fields given by retarded-potential integrals," in *16th AIAA/CEAS Aeroacoustics Conference* (2010).
[8]F. Margnat and V. Fortuné, "An iterative algorithm for computing aeroacoustic integrals with application to the analysis of free shear flows," J. Acoust. Soc. Am. **128**(4), 1656–1667 (2010).
[9]E. Heyman and A. J. Devaney, "Time-dependent multipoles and their application for radiation from volume source distributions," J. Math. Phys. **37**(2), 682–692 (1996).
[10]M. Frigo and S. G. Johnson, "The design and implementation of FFTW3," Proc. IEEE **93**(2), 216–231 (2005).
[11]N. Schaeffer, "Efficient spherical harmonic transforms aimed at pseudo-spectral numerical simulations," Geochem., Geophys. Geosyst. **14**(3), 751–758 (2013).
[12]J. E. Ffowcs Williams and D. L. Hawkings, "Sound generation by turbulence and surfaces in arbitrary motion," Philos. Trans. R. Soc., A **264**, 321–342 (1969).
[13]A. S. Lyrintzis, "Surface integral methods in computational aeroacoustics—From the (CFD) near-field to the (Acoustic) far-field," Int. J. Aeroacoust. **2**(2), 95–128 (2003).
[14]G. H. Golub and C. F. Van Loan, *Matrix Computations*, 3rd ed. (Johns Hopkins, Baltimore, MD, 1996).
[15]M. Kessler and S. Wagner, "Source-time dominant aeroacoustics," Comput. Fluids **33**, 791–800 (2004).